

# ROTATIONAL VARIABLES: *KEPLER* VERSUS ASAS-SN

JACK STETHEM<sup>1,\*</sup> , CHRISTOPHER S. KOCHAN<sup>1,2</sup> , ANYA PHILLIPS<sup>3</sup> , LYRA CAO<sup>4</sup> ,  
AND MARC PINSONNEAULT<sup>1</sup> 

<sup>1</sup>Department of Astronomy, The Ohio State University, 140 W 18th Ave, Columbus, OH 43210

<sup>2</sup>Center for Cosmology and AstroParticle Physics, 191 W Woodruff Ave, Columbus, OH 43210

<sup>3</sup>Center for Astrophysics | Harvard & Smithsonian, 60 Garden Street, Cambridge, MA 02138 and

<sup>4</sup>Department of Physics and Astronomy, Vanderbilt University, 6301 Stevenson Center Lane, Nashville, TN 37235

Version June 18, 2025

## ABSTRACT

Rotational variables are stars that vary in brightness due to star spots modulated by rotation. They are probes of stellar magnetism, binarity, and evolution. Phillips et al. (2024) explored distinct populations of  $\sim 50,000$  high-amplitude rotational variables from the All-Sky Automated Survey for Supernovae (ASAS-SN), examining correlations between stellar rotation, binarity, and activity. Here, we carry out a similar analysis of  $\sim 50,000$  much lower amplitude *Kepler* rotational variables. The *Kepler* population is dominated by slowly rotating, single, main sequence stars, with a striking absence of the rapidly rotating main sequence group in the ASAS-SN sample. The binary fractions of the *Kepler* rotators are significantly lower than for the ASAS-SN systems and they are significantly less spotted, as expected from their lower amplitudes. The scope of these statistical surveys will dramatically increase in the near future.

## 1. INTRODUCTION

Rotating stars with convective envelopes generate magnetic fields which then produce star spots at the surface (see the review by Strassmeier 2009). Since the distribution of these spots is not uniform, the light curve of the star varies with the period of rotation, giving rise to the class of rotational variable stars. Because the spot patterns evolve over time, the light curves also evolve and are not strictly periodic. Magnetically active main sequence stars lie at temperatures below the Kraft (1967) break where the convective zones of hotter stars becomes too thin to support significant magnetic activity and winds. For these active stars, the magnetic activity then declines with age because angular momentum loss through winds slows the rotation (Skumanich 1972).

This leads to a trend of slower rotation for greater ages that can be used to estimate stellar ages through “gyrochronology” (e.g., Epstein & Pinsonneault 2014, Angus et al. 2019, Bouma et al. 2023). Stars in sufficiently close binaries avoid spinning down by becoming tidally locked at the orbital period and can maintain their magnetic activity throughout their main sequence life time (Wilson 1966). For binaries with sufficiently short orbital periods, continued angular momentum loss through stellar winds can lead to a merger and a rejuvenated, rapidly rotating single star (Andronov et al. 2006).

Evolved stars should generally rotate slowly and be relatively inactive because of both the earlier angular momentum losses and the consequences of expansion and angular momentum conservation. Binary tidal interactions and mergers can lead to faster rotation and more activity (see, e.g., Massarotti et al. 2008, Carlberg et al.

2011, Tayar et al. 2015, Daher et al. 2022, Patton et al. 2023). Known populations of rapidly rotating, synchronized binaries are the RS CVn stars (Hall 1976) and the sub-subgiants (Leiner et al. 2022).

Phillips et al. (2024) analyzed  $\sim 50,000$  high-amplitude ( $\gtrsim 0.03$  mag) rotational variables in the All-Sky Automated Survey for Supernovae (ASAS-SN, Shappee et al. 2014, Kochanek et al. 2017). These included previously known systems and systems identified by searches for variable stars in ASAS-SN (Jayasinghe et al. 2018, 2019a,b, 2020, 2021; Christy et al. 2023). Christy et al. (2023) noted that the rotational variables lay in distinct clusters in the space of period and absolute magnitude, and Phillips et al. (2024) explored this in detail. Using data from APOGEE (Apache Point Observatory Galactic Evolution Experiment) DR17 (Abdurro’uf et al. 2022) and *Gaia* DR3 (Gaia Collaboration et al. 2016, Gaia Collaboration et al. 2023), they could determine whether the initial classes consisted of single stars, binary stars or a mixture. As in Daher et al. (2022), the binaries were largely identified by having a sufficiently high scatter in repeated radial velocity (RV) measurements, although some orbital and rotational period comparisons could be made for *Gaia* DR3 stars with full orbital solutions (Gosset et al. 2024). They also examined the spot covering fractions using the method of Cao & Pinsonneault (2022).

There were three main sequence groups. MS1 consisted of relatively slowly rotating single stars with periods of  $P_{\text{rot}} \sim 10\text{--}30$  days. MS2s consisted of single stars that are more rapidly rotating ( $\lesssim 10$  days), while MS2b consisted of tidally locked binary stars with similar periods. There were four groups of giants. The G1/G3 stars were heavily spotted, tidally locked RS CVn stars with periods

\*Corresponding author: stethem.5@buckeyemail.osu.edu

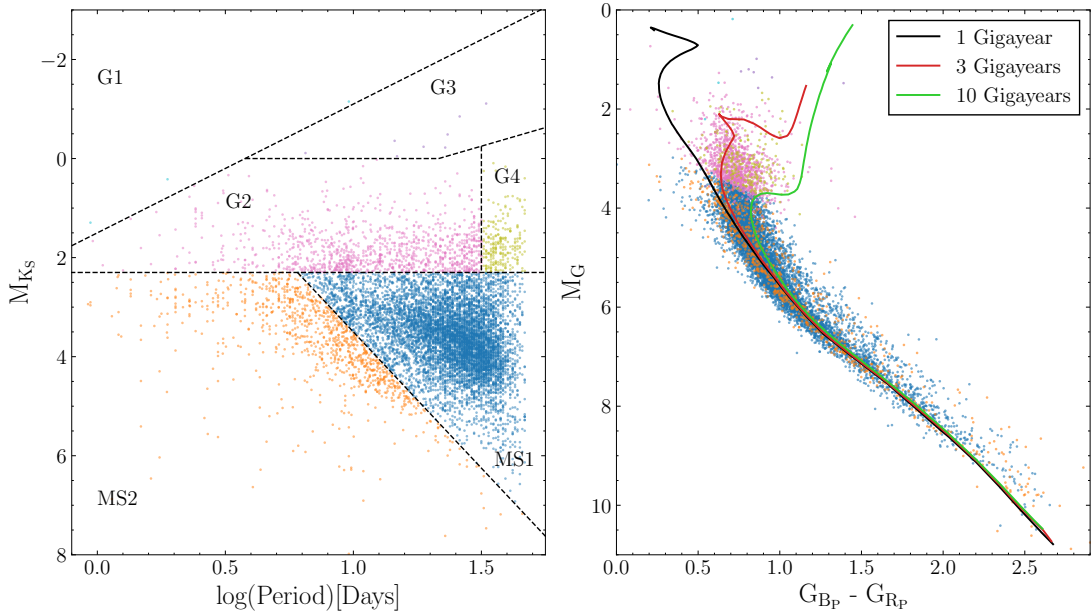


FIG. 1.— (Left panel) Distribution of a random 15 percent of the *Kepler* stars in absolute  $K_S$  magnitude and period along with the rotational variable class boundaries from Phillips et al. (2024). (Right panel) CMD of the same stars in absolute G magnitude and  $B_P - R_P$  color, color-coded by class. The curves are 1, 3, and 10 Gyr Solar metallicity PARSEC (Bressan et al. 2012; Marigo et al. 2013) isochrones.

TABLE 1  
STATISTICS OF THE KEPLER SAMPLE

	Total	MS1	MS2	G1	G2	G3	G4
Gaia	55107	41510	5717	45	6529	30	1276
Gaia w/ Orbital Solutions	501	302	51	0	129	2	17
APOGEE	2496	1519	292	4	365	4	49
APOGEE w/ Amplitudes	906	496	199	1	107	1	4

of tens of days. The G2 stars were less luminous, heavily spotted, tidally locked, sub-subgiants with periods  $\sim 10$  days. The G4s group consisted of single stars with luminosities intermediate to the G1/3 and G2 groups and slow rotation periods (approaching 100 days) that were almost certainly merger remnants. The G1/G3 groups were combined because the G1 stars seemed to simply be G3 stars where the periodograms favor finding  $P_{rot}/2$ . The G4b stars had similar periods to the G4s stars, but consisted of sub-synchronously rotating binaries.

ASAS-SN uniformly studied the variability of all bright stars with a roughly daily cadence over a long time baseline and a sensitivity of  $\sim 0.03$  mag. *Kepler* (Borucki et al. 2010, Koch et al. 2010), by contrast, provided exquisite photometric precision and high cadence observations of stars chosen to optimize planet searches in a small, fixed field off the Galactic plane. It was used to identify large samples of primarily main sequence and sub-giant rotational variables (e.g., McQuillan et al. 2014, Santos et al. 2019, Reinhold et al. 2023). The *Kepler* rotational variables essentially all have amplitudes of  $\lesssim 0.03$  mag that are disjoint from the amplitudes of the ASAS-SN sample. Daher et al. (2022) identified binaries in *Kepler* using APOGEE estimates of the stellar rotation rate  $v \sin i$  as a second variable. Massarotti et al. (2008), Carlberg et al. (2011), Tayar et al. (2015) and Patton et al. (2023) also explored the binarity of rapidly rotating spotted giants.

The complementary properties of ASAS-SN and *Ke-*

*pler* highlight the potential value of comparing their similarly sized populations of rotational variables. Here we carry out a similar analysis to Phillips et al. (2024) for  $\sim 50,000$  *Kepler* rotational variables from McQuillan et al. (2014) and Reinhold et al. (2023). The latter includes samples considered by Santos et al. (2019). In Section 2, we describe the data used in this study and its limitations. In Section 3, we examine the distribution of the *Kepler* rotational variables in class, binary properties (both fractions and tidal locking) and spot covering fractions in comparison to the Phillips et al. (2024) sample. Finally, in Section 4, we summarize and outline future directions.

## 2. OBSERVATIONS AND METHODS

We started from 67,163 rotational variables from *Kepler* (Borucki et al. 2010; Koch et al. 2010) with rotation periods from Reinhold et al. (2023). Reinhold et al. (2023) did not include amplitudes, so we used amplitudes from the subset of these stars in McQuillan et al. (2014). We cross-matched the stars to the *Gaia* DR3 (*Gaia* Collaboration et al. 2023) catalog, only keeping stars with *Gaia* parallax signal-to-noise ratios  $\varpi/\sigma_\varpi > 10$ . We then matched these stars with the APOGEE DR17 (Abdurro'uf et al. 2022) and 2MASS (Skrutskie et al. 2006) catalogs. We used distance estimates from Bailer-Jones et al. (2021) and the 3D ‘Combined 19’ MWDUST (Bovy et al. 2016) model to estimate extinctions. These models are based on the Drimmel et al. (2003), Marshall et al.

(2006) and Green et al. (2019) dust distributions.

We evaluated the binarity of the stars using the APOGEE DR17 and *Gaia* DR3 catalogs. Identifying binary companions is important because short-period binaries can undergo tidal interactions that alter their rotation rates. For example, tidally interacting binaries cannot be used for gyrochronology. APOGEE offers high-precision radial velocities, but only 2,496 stars in our sample have multiple RV measurements (NVIS-ITS > 1), as summarized in Table 1. Following Phillips et al. (2024), we flagged stars as binaries if their velocity scatter (VSCATTER) exceeded  $3 \text{ km s}^{-1}$ , a conservative threshold indicating likely binarity (Badenes et al. 2018). *Gaia* provides radial velocity measurements for a larger fraction of the sample but at significantly lower precision. Nevertheless, we flagged possible binaries using the `rv_amplitude_robust` >  $20 \text{ km s}^{-1}$  criterion and the quality filters from Katz et al. (2023):

1. `rv_nb.transits`  $\geq 5$ ,
2. `rv_expected_sig_to_noise`  $\geq 5$ , and
3.  $3900\text{K} \leq \text{rv\_template\_teff} \leq 8000\text{K}$

These thresholds ensure that we detect binaries with significant dynamical effects while minimizing contamination from noise. We also cross-matched our sample with the *Gaia* DR3 binary solutions from Gosset et al. (2024), identifying both SB1 and SB2 systems. For these systems we can compare the rotational and orbital periods to see if systems are tidally locked.

Finally, we used the star spot coverage estimates determined by the LEOPARD analysis of APOGEE spectra (Cao & Pinsonneault 2022). This algorithm fits the APOGEE spectrum using models with two different temperatures to estimate the temperature ratio  $X_{\text{spot}} = T_{\text{in}}/T_{\text{out}}$  between the regions in and out of spots and the spot coverage fraction,  $f_{\text{spot}}$ . If the side of the star we do not see has a spot fraction  $f'_{\text{spot}}$ , then the mean flux of the star satisfies

$$T_{\text{eff}}^4 = \frac{1}{2} (f_{\text{spot}} T_{\text{in}}^4 + (1 - f_{\text{spot}}) T_{\text{out}}^4) \quad (1)$$

$$+ \frac{1}{2} (f'_{\text{spot}} T_{\text{in}}^4 + (1 - f'_{\text{spot}}) T_{\text{out}}^4) \quad (2)$$

where  $T_{\text{eff}}$  is the effective temperature. The fractional change in flux relative to  $T_{\text{eff}}^4$  between the two sides of

$$v = \frac{\Delta f (1 - X_{\text{spot}}^4)}{1 - \langle f \rangle (1 - X_{\text{spot}}^4)} \quad (3)$$

is a proxy for the variability due to the spots, where  $\Delta f = |f_{\text{spot}} - f'_{\text{spot}}|$  is the difference in the spot fractions and  $\langle f \rangle = (f_{\text{spot}} + f'_{\text{spot}})/2$  is the mean spot fraction. The actual variability also depends on the stellar temperature and the observing band passes, but this is an unnecessary complication since we simply want to illustrate the differences between the samples. We will use  $v$  with  $f'_{\text{spot}} = 0$  ( $\Delta f = f_{\text{spot}}$ ,  $\langle f \rangle = f_{\text{spot}}/2$ ) to make the comparisons. One important caveat for the LEOPARD estimates of spot properties is that they can be biased if the star has a binary companion bright enough for the absorption lines of the companion to have an effect on the estimates of  $f_{\text{spot}}$  and  $X_{\text{spot}}$ .

### 3. DISCUSSION

Figure 1 shows the distributions of a random 15 percent of the stars in  $M_{K_s}$  and period and in a *Gaia* color-magnitude diagram (CMD). The stars are divided into the same classes as Phillips et al. (2024) using the boundaries shown in Figure 1. Table 1 gives the number of rotational variables from Reinhold et al. (2023) with *Gaia* magnitudes and parallax errors  $\sigma_{\varpi}/\varpi < 1/10$  divided into these groups. The *Kepler* samples focused on main sequence stars and, to a lesser extent, sub-giants, but generally avoided stars on the giant branch, as seen in Figure 1. The *Kepler* samples also discriminated against wider binaries, avoiding resolved systems or systems with large *Gaia* RUWE (Renormalized Unit Weight Error) where the astrometry residuals suggest the presence of a companion. There does not seem to be any significant discrimination against short period binaries (e.g. avoiding systems lying above the main sequence). Reinhold et al. (2023) only allowed rotational periods shorter than 50 days leading to the sharp edge in the period distribution. For these reasons, we focus on the MS and sub-giant systems with limited results for the more luminous giants.

The distribution of the MS stars in the left panel of Figure 1 is strikingly different from Phillips et al. (2024). Both samples have a clump of MS1 stars with a fairly well defined peak near a period of 25 days. But in the *Kepler* sample, the MS2 group is essentially absent and lacks a well defined peak.

In Phillips et al. (2024), only 14% of the MS stars belonged to the MS1 class, while here 88% of them belong to MS1. This cannot simply be an unrecognized bias against short period binaries in *Kepler*. The MS1 and MS2 binary fractions in Phillips et al. (2024) were 4.3% and 34.3%, respectively, and if we correct our current numbers for losing these fractions, the corrected ratio would be that 83% of the *Kepler* stars are in MS1. Moreover, the MS2 systems have shorter periods (<10 days) than the MS1 systems and the MS2 binaries in Phillips et al. (2024) were tidally locked, so any biases against binaries in *Kepler* would do little to their inclusion.

Figure 2 shows the distribution of the MS1, MS2, G2 and G4 classes in *Gaia* `rv_amplitude_robust` and APOGEE VSCATTER as compared to the equivalent distributions from Phillips et al. (2024). The MS1 rotators are again overwhelmingly dominated by single stars with VSCATTER and `rv_amplitude_robust` distributions that are very similar to the MS1 rotators in Phillips et al. (2024). The *Kepler* MS2 distributions are very different, with much lower binary fractions than in Phillips et al. (2024). While the *Kepler* MS2 systems have a tail to higher velocity scatters, only 8.9% of the systems have a VSCATTER > 3 km/s as compared to 34.3% in the Phillips et al. (2024) sample. That the distribution shows a peak at the highest values of VSCATTER strongly suggests that there are real binaries in the *Kepler* MS2 group. If we define  $x \equiv v_{\text{obs}}/v_{\text{max}}$  as the ratio of the scatter that would be observed edge on to the scatter  $v_{\text{obs}} = v_{\text{max}} \sin i$  that would be observed at inclination  $i$ , then the probability distribution of  $x$  for random inclinations is  $x(1-x^2)^{-1/2}$  which peaks for  $v_{\text{obs}} \rightarrow v_{\text{max}}$ , similar to what we see in Figure 2.

Simonian et al. (2019) examined the binary fraction

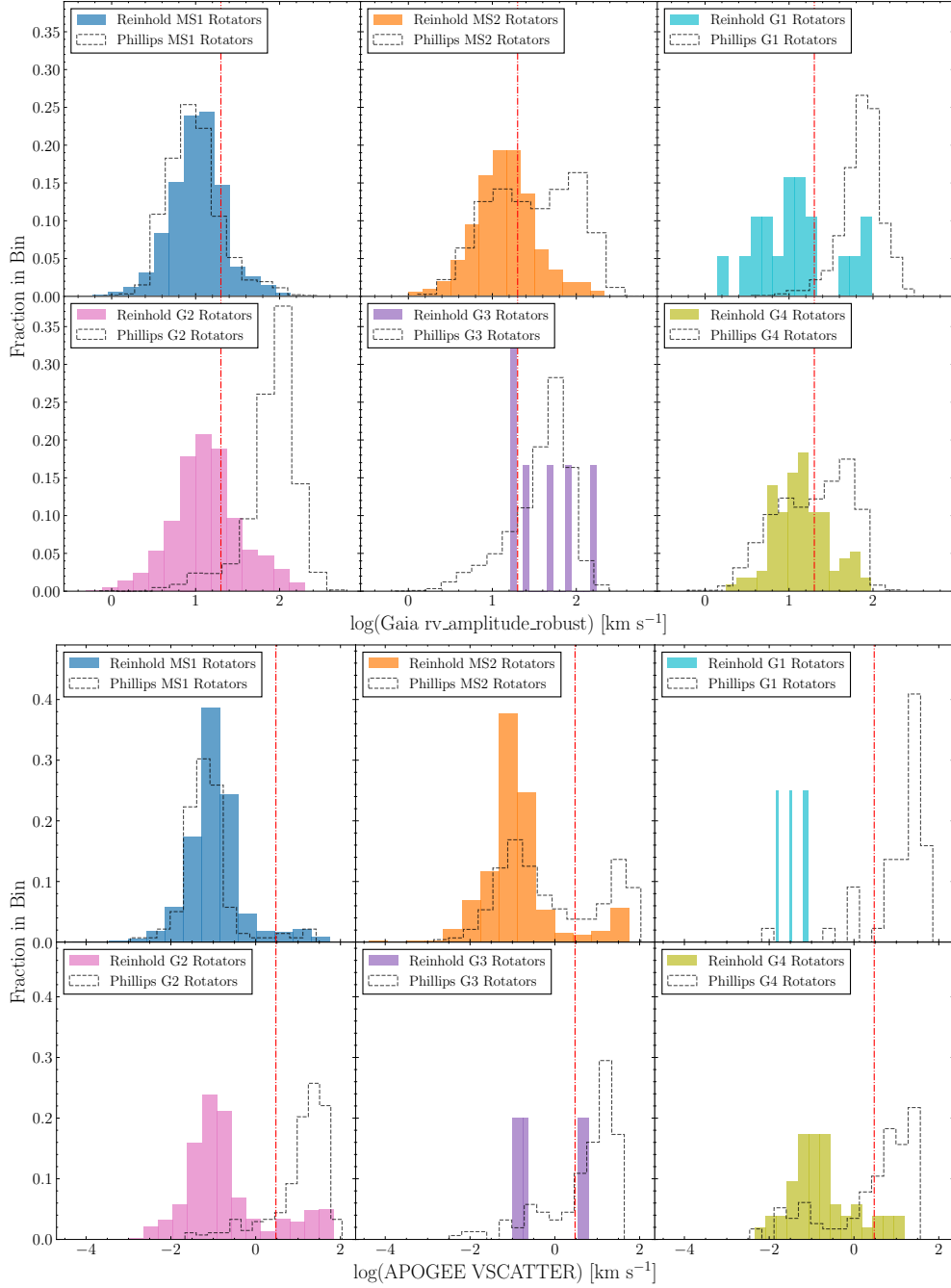


FIG. 2.— Distributions of the MS1, MS2, G2, and G4 *Kepler* stars in *Gaia* *rv\_amplitude\_robust* (top panels) and APOGEE VSCATTER (bottom panels). Rotators to the right of the vertical lines at 20 km s<sup>−1</sup> (top panels) and 3 km s<sup>−1</sup> (bottom panels) are almost certainly binaries.

of the rapidly rotating ( $1.5 < P < 7$  day) McQuillan et al. (2014) rotational variables using magnitude offsets from the main sequence. Figure 3 shows a version of this using the offset of fixed color ( $\Delta M_g$ ) between the MS1/MS2 stars and a 3 Gyr PARSEC (Bressan et al. 2012; Marigo et al. 2013) isochrone for the stars which can be flagged as binaries using either *Gaia* or APOGEE velocity scatters. If the distribution of mass ratios  $q$  is uniform, and the main sequence luminosity scales as mass  $M^a$  with  $a = 3$ -4, the distribution in  $x = \Delta M_g$  is

$$\frac{dP}{dx} \propto 10^{-0.4x} (10^{-0.4x} - 1)^{1/a-1} \quad (4)$$

is quite flat despite the singularity if smoothed over even  $\Delta M_g = 0.1$ . For  $a = 3$ , the binary fraction rises by roughly a factor of two from nearly equal-mass binaries ( $\Delta M_g = -1.5$ ) to systems with low-mass companions ( $\Delta M_g \rightarrow 0$ ). Given the crudeness of our estimate of  $\Delta M_g$  (see Simonian et al. (2019) for a more detailed treatment) and the modest sample size, this is broadly consistent with the binary distributions shown in Figure 3. While Simonian et al. (2019) report a significantly higher binary fraction (59%) than we find for the main sequence population as a whole, their analysis focused on very rapidly rotating stars. Our binary

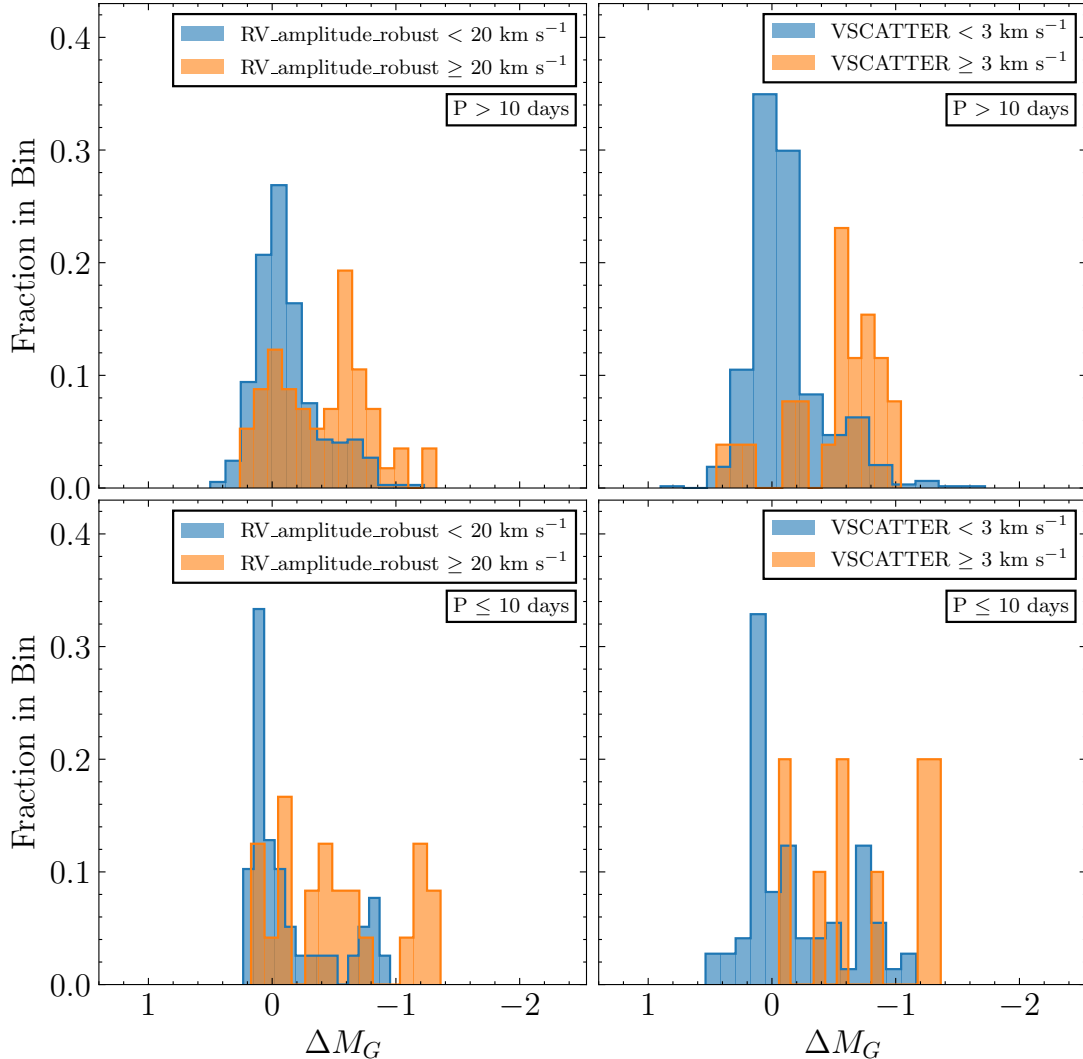


FIG. 3.— Distribution of the  $\Delta M_G$  offset between a star’s  $M_G$  absolute magnitude and the three gigayear parsec isochrons (Bressan et al. 2012; Marigo et al. 2013). For both the MS1 and MS2 stars, the bottom (top) two panels display the distribution for stars with periods shorter (longer) than 10 days.

fractions also are not corrected for completeness due to inclination effects and the RV sampling simply missing phases with large velocity differences. The first effect is small even if the true VSCATTER is only modestly above the  $3 \text{ km s}^{-1}$  limit (it includes  $> 90\%$  of systems with equatorial  $VSCATTER = 6 \text{ km/s}$ ). The effects of the phase sampling are likely larger for smaller numbers of APOGEE visits, but a full statistical correction of the phase sampling would be a significant Monte Carlo modeling project. The panels in Figure 3 separate the distributions by rotation period, highlighting this distinction: among stars with  $P \leq 10$  days, we find a binary fraction of 12.1% (38.1%) using VSCATTER (rv\_amplitude\_robust), compared to just 3.9% (13.3%) for the slower rotators. This trend is qualitatively consistent with the findings of Simonian et al. (2019), who also observed a higher binary fraction among the most rapidly rotating systems.

In Phillips et al. (2024), the lower luminosity G2 and G4 classes are dominated by binaries, although G4 had a minority population of single stars. As we see in Fig-

ure 2, this is completely reversed for the *Kepler* stars. Both groups are dominated by single stars with a minority of binaries. For example 84.9% (63.5%) of G2 (G4) stars had VSCATTER  $> 3 \text{ km/s}$  in Phillips et al. (2024), while only 16.1% (11.5%) of the *Kepler* stars have such large VSCATTER values. For the more luminous giants, G1 has a sufficient number of *Gaia* RV\_amplitude\_robust measurements to make a clear comparison, and we find that the *Kepler* stars are primarily single stars while the Phillips et al. (2024) stars are mostly binaries. For the G3 giants, there are too few *Kepler* stars with velocity information to make a comparison.

In addition to the abundance of binaries, we are also interested in whether the systems are tidally locked, with rotational periods  $P_{rot}$  equal to their orbital periods  $P_{orb}$ . We can make the comparison for the limited number of systems with orbital solutions in *Gaia* DR3 (Gosset et al. 2024) with the caveat that we have found significant fractions of period mismatches between ASAS-SN photometric periods and *Gaia* DR3 orbital periods in eclipsing binaries (e.g, Rowan et al. 2023). Here we use the criteria



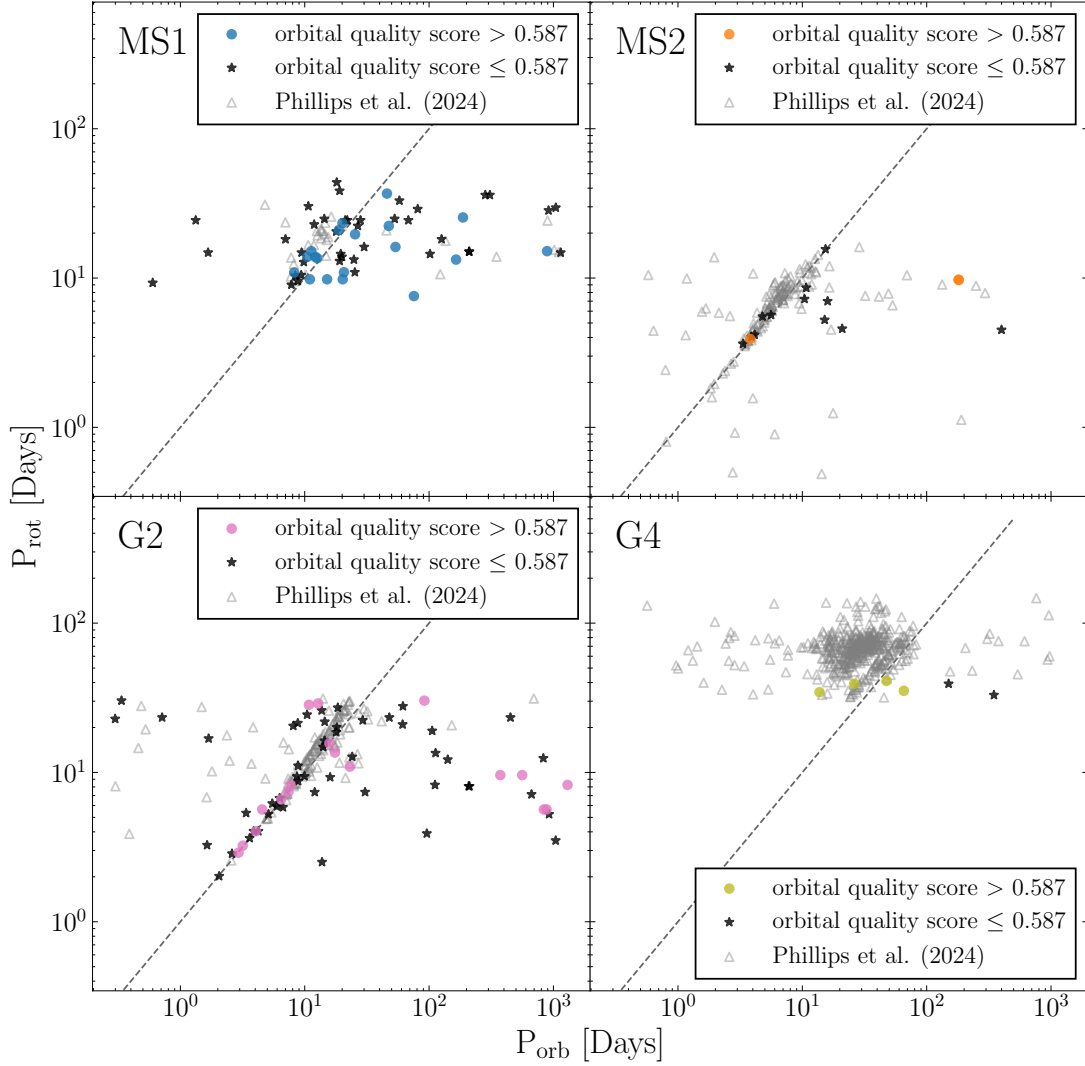


FIG. 4.— The [Reinhold et al. \(2023\)](#) rotational period  $P_{rot}$  compared to the *Gaia* orbital period  $P_{orb}$ . Tidally locked systems would lie on the dashed line with  $P_{rot} = P_{orb}$ . The orbital quality scores use the criteria in [Bashi et al. \(2022\)](#)

of [Bashi et al. \(2022\)](#) to flag potentially bad orbital solutions. Figure 4 compares the two periods for the MS1, MS2, G2 and G4 groups - there are too few G1 and G3 stars with orbital solutions to make a comparison.

[Phillips et al. \(2024\)](#) had too few MS1 systems with *Gaia* orbits to draw strong conclusions, while the binary MS2 systems were dominated by tidally synchronized systems. For the *Kepler* stars, the majority of MS1 binary systems are not tidally synchronized and the orbital periods are much longer than the rotational periods. The gap in the orbital periods near one year is due to the *Gaia* scanning patterns. There does seem to be a minority of systems clustered near, but not on, the  $P_{orb} = P_{rot}$  line. This scatter is likely real since in the [Phillips et al. \(2024\)](#) samples (and for G2 here) there are populations where the two periods are much more similar. The MS2 binaries are also dominated by non-synchronous systems, but now with a minority lying on or close to the  $P_{orb} = P_{rot}$  line. In both samples, the periods of the synchronized systems are  $\sim 10$  days or lower. The G2 systems in [Phillips et al. \(2024\)](#) were essentially all tidally synchronized binaries, while the G4 systems were dominated by

sub-synchronous ( $P_{rot} > P_{orb}$ ) systems. Only  $\sim 1/4$  of the *Kepler* G2 systems are (close to) synchronous, while none of the G4 systems are synchronous. The G4 systems also almost all have  $P_{orb} > P_{rot}$  rather than the reverse.

As discussed earlier, there is an enormous difference in the variability amplitudes of the ASAS-SN and *Kepler* samples. Figure 5 shows the APOGEE binary fractions of the *Kepler* and ASAS-SN MS1 and MS2 stars in amplitude and period. As noted above, the binary fractions are not corrected for completeness, but the corrections should be roughly the same in each period bin. For both classes and populations, binary fractions increase with amplitude and decrease with period. The MS1 rotators from *Kepler* generally have higher binary fractions than the MS1 rotators from [Phillips et al. \(2024\)](#) despite their lower amplitudes, and this is also seen for each of the overlapping period bins. The MS2 rotators show a steadily increasing binary fraction with amplitude across both samples. At fixed periods, the binary fractions of the higher amplitude rotators are larger, and the *Kepler* population has none of the very short period (sub-day)

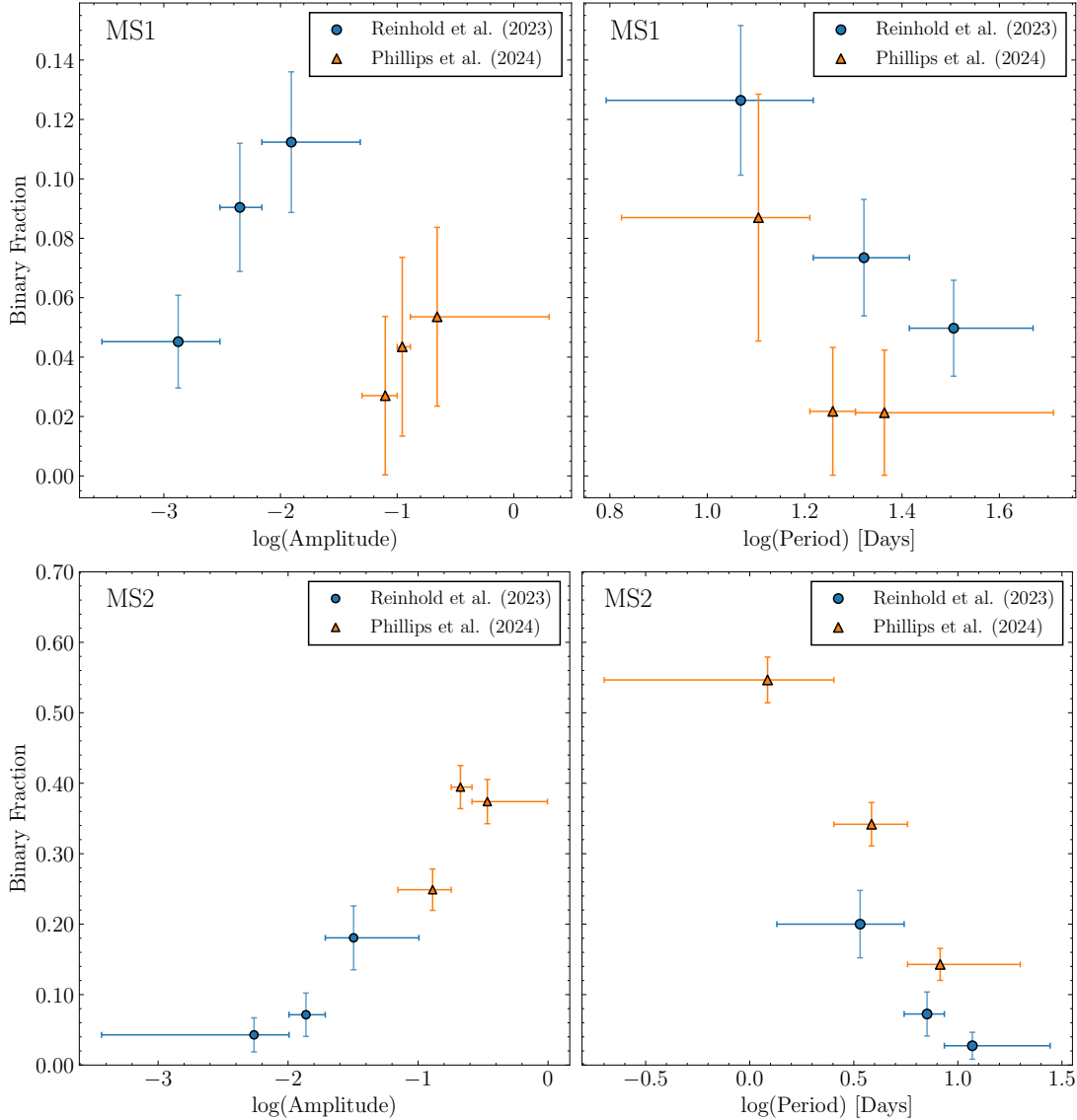


FIG. 5.— Binary fractions of MS1 (top panels) and MS2 (bottom panels) rotational variables from both *Kepler* and Phillips et al. (2024) in amplitude (left) and period (right). Each amplitude and period bin contains an equal number of stars.

systems seen in the Phillips et al. (2024) sample. There were not enough systems in the giant classes to do a similar analysis.

Figure 6 presents the integral distributions of the MS1 and MS2 groups in spot coverage fraction ( $f_{spot}$ ), temperature ratio ( $X_{spot}$ ) and variability ( $v$ , Eqn. 3) for the *Kepler* and Phillips et al. (2024) samples. The ASAS-SN systems generally have larger temperature differences and larger spot fractions, leading to larger estimates of the variability. For the MS1 group, the temperature ratios are quite similar between the samples, with larger differences in the spot fractions. For the MS2 group, the differences in both temperature and spot fractions are larger. The binary systems, are more spotted in both samples, with the caveat that the Cao & Pinsonneault (2022) estimates can be skewed by the spectral contributions of the secondary.

While the ASAS-SN stars are predicted to be more variable based on the spot models, the modeled amplitude differences remain significantly smaller than the ob-

served order-of-magnitude difference in variability. The estimates used in Figure 6 assume a limiting case where only the observed side of the star contains spots ( $f'_{spot} = 0$ ). To reconcile this with the much lower observed amplitudes in the *Kepler* sample, the stars would need not only smaller spot coverage fractions and lower temperature contrasts, but also more uniformly distributed spots across their surfaces. In the framework of Eqn. 3, this corresponds to  $f_{spot} \simeq f'_{spot}$ , yielding a small  $\Delta f$  and thus reduced photometric variability.

To illustrate this, we considered a simple toy model in which  $N$  identical spots are randomly distributed across two hemispheres of a star. The fractional difference in spot coverage between the hemispheres,  $\Delta f / \langle f \rangle$ , decreases with increasing  $N$ , approximately scaling as  $1/\sqrt{N}$  for large  $N$ . For example, the median fractional asymmetry is  $\Delta f / \langle f \rangle \sim 0.4$  for  $N = 10$  spots, but drops to  $\sim 0.04$  for  $N = 300$  spots. Thus, to maintain the low amplitudes observed in the *Kepler* sample, stars would

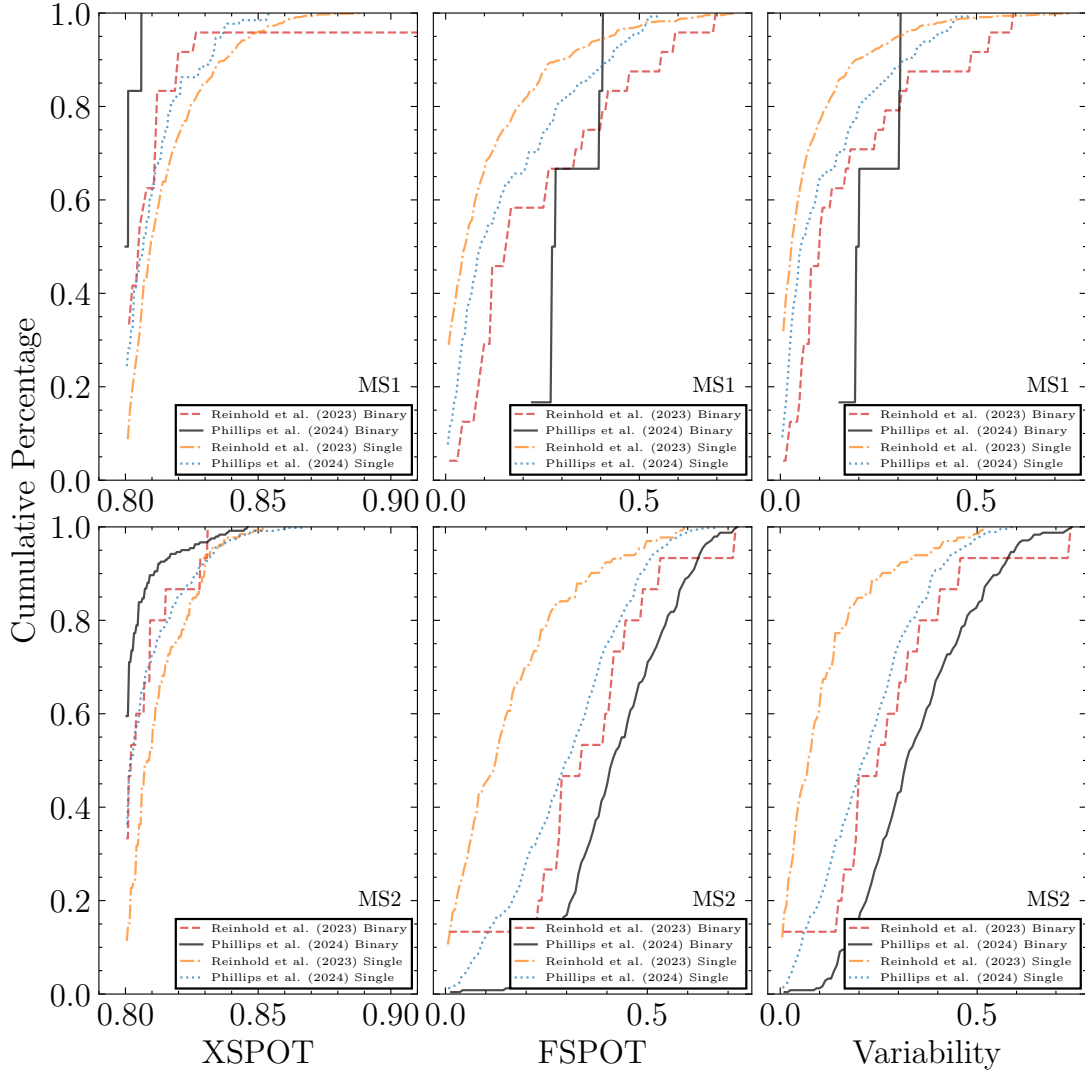


FIG. 6.— Integral distributions of the XSPOT, FSPOT, and variability  $v$  (Eqn. 3) for the main sequence Reinhold et al. (2023) and Phillips et al. (2024) binaries and single stars. This variability roughly corresponds to the fractional amplitude if only the “observed” side of the star is spotted.

either require an order of magnitude more (and likely smaller) spots than typical ASAS-SN stars, or the true spot distributions must be more uniform than assumed. There are limits to this argument since there is evidence that spot distributions in close binaries may not be random and can exhibit latitudinal or longitudinal preferences (Sethi & Martin 2024).

#### 4. CONCLUSION

As discussed in the introduction, Phillips et al. (2024) analyzed the clusters of rotational variables in absolute magnitude and period found by Christy et al. (2023) for their binary properties and star spot coverage fractions. Here we carry out a similar analysis of the much lower variability amplitude rotational variables from Kepler, using the results from Reinhold et al. (2023) and McQuillan et al. (2014). The *Kepler* samples contain very few of the higher luminosity giant rotator groups G1 and G3, so we focus on the MS groups and the less luminous G2 and G4 giant groups. In general, there are significant differences between the two samples for all of the groups.

**MS1:** The first striking result is that the longer period MS1s group dominates the *Kepler* sample, with 88% of the main sequence stars, compared to only 14% in Phillips et al. (2024). These stars are predominantly single in both samples and have modest binary fractions ( $\lesssim 10\%$ ) that increase with variability amplitude and decrease with rotation period. The *Kepler* sample has modestly higher binary fractions despite the lower amplitudes, but typically at longer periods. The majority of the *Kepler* binaries in this group are far from tidal synchronization.

The *Kepler* stars exhibit lower spot coverage fractions and slightly smaller temperature contrasts compared to the ASAS-SN sample. However, these differences are not sufficient to explain the significantly lower variability amplitudes observed in *Kepler* light curves. This implies that many of these stars must host a greater number of more symmetrically distributed spots, which would suppress variability without requiring low total spot coverage.

Several factors likely contribute to this discrepancy.



The *Kepler* field was chosen to contain an older stellar population, making rapidly rotating, highly active stars intrinsically rare in the sample. Stellar rotation also slows substantially over time, so the majority of stars in the *Kepler* field are expected to be older and magnetically inactive, with correspondingly low spot coverage. In contrast, ASAS-SN is biased toward detecting high-amplitude variability in bright stars, favoring the inclusion of more active systems with asymmetric spot distributions. Moreover, the *Kepler* target selection prioritized stars suitable for detecting transiting exoplanets, and this process may have implicitly excluded or de-emphasized active stars, further shaping the sample’s variability properties.

**MS2:** In the Phillips et al. (2024) sample, the MS2 group has comparable numbers of MS2s single stars and MS2b binary stars, with the binaries largely being tidally synchronized. For the *Kepler* stars, there are many fewer binaries and most are not tidally synchronized. The binary fraction is less than 1/2 that of the Phillips et al. (2024) sample, with a smooth trend of binary fraction with variability amplitude across both samples (Figure 5). The temperature contrasts and spot fraction differences (Figure 6) are larger for the MS2 stars, but the amplitude differences again seem to require that the *Kepler* stars have many more spots.

**G2 and G4:** In Phillips et al. (2024), these sub-giant stars are essentially all tidally locked binaries. In *Kepler* they are mostly single stars, while the binaries are a mixture of tidally locked binaries and systems with  $P_{orb} \gg P_{rot}$ . These sub-giant groups show pronounced differences between the two samples. The Phillips et al. (2024) G4 systems are mostly sub-synchronously rotating binaries with a modest fraction of single stars. In *Kepler* they are almost all single stars, and those in binaries have orbital periods uncorrelated with the rotation periods. There were too few *Kepler* stars with spot fraction estimates to make a comparison.

Since tidally locked stars generally have short rotational periods, it is not surprising that the high variability amplitude ASAS-SN systems systematically show larger binary populations than the low amplitude *Kepler* systems. However, APOGEE is sensitive to quite wide binaries ( $\sim 3000$  days, see Daher et al. 2022), and most of this period range would not lead to tidal interactions. The spot statistics for the binaries should be interpreted with caution, however, because spectral lines from the convergence can skew the spot statistics. The *Kepler* stars are generally non-synchronous binaries, particularly in the MS1 and MS2 classes, with synchronization restricted to shorter orbital periods ( $\lesssim 10$  days). This contrasts with the tidal synchronization observed in many Phillips et al. (2024) binaries.

Across both samples, higher variability amplitudes correspond to increased binary fractions, underscoring the interplay between binarity, magnetic activity, and rotational evolution. Binary systems have higher spot coverage fractions ( $f_{spot}$ ) but, the *Kepler* binaries have slightly lower values than their counterparts in Phillips et al. (2024).

There is considerable scope for expanding population studies of rotational variables. First, there will be larger samples of low amplitude rotational stars identified by TESS (Transiting Exoplanets Survey Satellite) (e.g.,

Claytor et al. 2022, Holcomb et al. 2022, Colman et al. 2024), with the caveat that the TESS observing strategy makes it difficult to identify longer period ( $\gtrsim 2$  weeks) systems. Ground based variability surveys like ASAS-SN will continue to expand the samples of higher amplitude systems, and will be able to identify lower amplitude systems as the light curves extend in time.

The real limitation on population studies is the small fraction with good binary discrimination or binary orbit solutions. While the *Gaia* `rv_amplitude_robust` is available for most of these stars, it is only sensitive to scatters  $> 20$  km/s, and only a tiny fraction of the systems have full *Gaia* orbital solutions. Fortunately, the number of systems with orbital solutions should expand by over an order of magnitude with *Gaia* DR4. SDSS Milky Way Mapper (see Kollmeier et al. 2017) will greatly increase the number of systems with APOGEE’s higher precision velocity scatters. As shown by Phillips & Kochanek (2025), the velocity scatter distributions can be used to statistically estimate the primary masses and secondary mass ratios even without having a full orbit solution.

CSK is supported by NSF grants AST-2307385 and AST-2407206. AP is supported by the National Science Foundation Graduate Research Fellowship under Grant No. DGE 2140743. MHP and LC acknowledge support from NASA grant 80NSSC23K0205.

## REFERENCES

- Abdurro'uf, Accetta, K., Aerts, C., et al. 2022, *ApJS*, 259, 35, doi: [10.3847/1538-4365/ac4414](https://doi.org/10.3847/1538-4365/ac4414)
- Andronov, N., Pinsonneault, M. H., & Terndrup, D. M. 2006, *ApJ*, 646, 1160, doi: [10.1086/505127](https://doi.org/10.1086/505127)
- Angus, R., Morton, T. D., Foreman-Mackey, D., et al. 2019, *AJ*, 158, 173, doi: [10.3847/1538-3881/ab3c53](https://doi.org/10.3847/1538-3881/ab3c53)
- Badenes, C., Mazzola, C., Thompson, T. A., et al. 2018, *ApJ*, 854, 147, doi: [10.3847/1538-4357/aaa765](https://doi.org/10.3847/1538-4357/aaa765)
- Bailer-Jones, C. A. L., Rybizki, J., Fouesneau, M., Demleitner, M., & Andrae, R. 2021, *AJ*, 161, 147, doi: [10.3847/1538-3881/abd806](https://doi.org/10.3847/1538-3881/abd806)
- Bashi, D., Shahaf, S., Mazeh, T., et al. 2022, *MNRAS*, 517, 3888, doi: [10.1093/mnras/stac2928](https://doi.org/10.1093/mnras/stac2928)
- Borucki, W. J., Koch, D., Basri, G., et al. 2010, *Science*, 327, 977, doi: [10.1126/science.1185402](https://doi.org/10.1126/science.1185402)
- Bouma, L. G., Palumbo, E. K., & Hillenbrand, L. A. 2023, *ApJ*, 947, L3, doi: [10.3847/2041-8213/acc589](https://doi.org/10.3847/2041-8213/acc589)
- Bovy, J., Rix, H.-W., Green, G. M., Schlafly, E. F., & Finkbeiner, D. P. 2016, *ApJ*, 818, 130, doi: [10.3847/0004-637X/818/2/130](https://doi.org/10.3847/0004-637X/818/2/130)
- Bressan, A., Marigo, P., Girardi, L., et al. 2012, *MNRAS*, 427, 127, doi: [10.1111/j.1365-2966.2012.21948.x](https://doi.org/10.1111/j.1365-2966.2012.21948.x)
- Cao, L., & Pinsonneault, M. H. 2022, *MNRAS*, doi: [10.1093/mnras/stac2706](https://doi.org/10.1093/mnras/stac2706)
- Carlberg, J. K., Majewski, S. R., Patterson, R. J., et al. 2011, *ApJ*, 732, 39, doi: [10.1088/0004-637X/732/1/39](https://doi.org/10.1088/0004-637X/732/1/39)
- Christy, C. T., Jayasinghe, T., Stanek, K. Z., et al. 2023, *MNRAS*, 519, 5271, doi: [10.1093/mnras/stac3801](https://doi.org/10.1093/mnras/stac3801)
- Claytor, Z. R., van Saders, J. L., Llama, J., et al. 2022, *ApJ*, 927, 219, doi: [10.3847/1538-4357/ac498f](https://doi.org/10.3847/1538-4357/ac498f)
- Colman, I. L., Angus, R., David, T., et al. 2024, *AJ*, 167, 189, doi: [10.3847/1538-3881/ad2c86](https://doi.org/10.3847/1538-3881/ad2c86)
- Daher, C. M., Badenes, C., Tayar, J., et al. 2022, *MNRAS*, 512, 2051, doi: [10.1093/mnras/stac590](https://doi.org/10.1093/mnras/stac590)
- Drimmel, R., Cabrera-Lavers, A., & López-Corredoira, M. 2003, *A&A*, 409, 205, doi: [10.1051/0004-6361:20031070](https://doi.org/10.1051/0004-6361:20031070)
- Epstein, C. R., & Pinsonneault, M. H. 2014, *ApJ*, 780, 159, doi: [10.1088/0004-637X/780/2/159](https://doi.org/10.1088/0004-637X/780/2/159)
- Gaia Collaboration, Prusti, T., de Bruijne, J. H. J., et al. 2016, *A&A*, 595, A1, doi: [10.1051/0004-6361/201629272](https://doi.org/10.1051/0004-6361/201629272)
- Gaia Collaboration, Vallenari, A., Brown, A. G. A., et al. 2023, *A&A*, 674, A1, doi: [10.1051/0004-6361/202243940](https://doi.org/10.1051/0004-6361/202243940)
- Gosset, E., Damerdj, Y., Morel, T., et al. 2024, *arXiv e-prints*, *arXiv:2410.14372*, doi: [10.48550/arXiv.2410.14372](https://doi.org/10.48550/arXiv.2410.14372)
- Green, G. M., Schlafly, E., Zucker, C., Speagle, J. S., & Finkbeiner, D. 2019, *ApJ*, 887, 93, doi: [10.3847/1538-4357/ab5362](https://doi.org/10.3847/1538-4357/ab5362)
- Hall, D. S. 1976, in *Astrophysics and Space Science Library*, Vol. 60, IAU Colloq. 29: Multiple Periodic Variable Stars, ed. W. S. Fitch, 287, doi: [10.1007/978-94-010-1175-4\\_15](https://doi.org/10.1007/978-94-010-1175-4_15)
- Holcomb, R. J., Robertson, P., Hartigan, P., Oelkers, R. J., & Robinson, C. 2022, *ApJ*, 936, 138, doi: [10.3847/1538-4357/ac8990](https://doi.org/10.3847/1538-4357/ac8990)
- Jayasinghe, T., Kochanek, C. S., Stanek, K. Z., et al. 2018, *MNRAS*, 477, 3145, doi: [10.1093/mnras/sty838](https://doi.org/10.1093/mnras/sty838)
- Jayasinghe, T., Stanek, K. Z., Kochanek, C. S., et al. 2019a, *MNRAS*, 486, 1907, doi: [10.1093/mnras/stz844](https://doi.org/10.1093/mnras/stz844)
- . 2019b, *MNRAS*, 485, 961, doi: [10.1093/mnras/stz444](https://doi.org/10.1093/mnras/stz444)
- . 2020, *MNRAS*, 491, 13, doi: [10.1093/mnras/stz2711](https://doi.org/10.1093/mnras/stz2711)
- Jayasinghe, T., Kochanek, C. S., Stanek, K. Z., et al. 2021, *MNRAS*, 503, 200, doi: [10.1093/mnras/stab114](https://doi.org/10.1093/mnras/stab114)
- Katz, D., Sartoretti, P., Guerrier, A., et al. 2023, *A&A*, 674, A5, doi: [10.1051/0004-6361/202244220](https://doi.org/10.1051/0004-6361/202244220)
- Koch, D. G., Borucki, W. J., Basri, G., et al. 2010, *ApJ*, 713, L79, doi: [10.1088/2041-8205/713/2/L79](https://doi.org/10.1088/2041-8205/713/2/L79)
- Kochanek, C. S., Shappee, B. J., Stanek, K. Z., et al. 2017, *PASP*, 129, 104502, doi: [10.1088/1538-3873/aa80d9](https://doi.org/10.1088/1538-3873/aa80d9)
- Kollmeier, J. A., Zasowski, G., Rix, H.-W., et al. 2017, *arXiv e-prints*, *arXiv:1711.03234*, doi: [10.48550/arXiv.1711.03234](https://doi.org/10.48550/arXiv.1711.03234)
- Kraft, R. P. 1967, *ApJ*, 150, 551, doi: [10.1086/149359](https://doi.org/10.1086/149359)
- Leiner, E. M., Geller, A. M., Gully-Santiago, M. A., Gosnell, N. M., & Tofflemire, B. M. 2022, *ApJ*, 927, 222, doi: [10.3847/1538-4357/ac53b1](https://doi.org/10.3847/1538-4357/ac53b1)
- Marigo, P., Bressan, A., Nanni, A., Girardi, L., & Pumo, M. L. 2013, *MNRAS*, 434, 488, doi: [10.1093/mnras/stt1034](https://doi.org/10.1093/mnras/stt1034)
- Marshall, D. J., Robin, A. C., Reylé, C., Schultheis, M., & Picaud, S. 2006, *A&A*, 453, 635, doi: [10.1051/0004-6361:20053842](https://doi.org/10.1051/0004-6361:20053842)
- Massarotti, A., Latham, D. W., Stefanik, R. P., & Fogel, J. 2008, *AJ*, 135, 209, doi: [10.1088/0004-6256/135/1/209](https://doi.org/10.1088/0004-6256/135/1/209)
- McQuillan, A., Mazeh, T., & Aigrain, S. 2014, *ApJS*, 211, 24, doi: [10.1088/0067-0049/211/2/24](https://doi.org/10.1088/0067-0049/211/2/24)
- Patton, R. A., Pinsonneault, M. H., Cao, L., et al. 2023, *arXiv e-prints*, *arXiv:2303.08151*, <https://arxiv.org/abs/2303.08151>
- Phillips, A., & Kochanek, C. S. 2025, *Monthly Notices of the Royal Astronomical Society*, 539, 2608, doi: [10.1093/mnras/staf634](https://doi.org/10.1093/mnras/staf634)
- Phillips, A., Kochanek, C. S., Jayasinghe, T., et al. 2024, *MNRAS*, 527, 5588, doi: [10.1093/mnras/stad3564](https://doi.org/10.1093/mnras/stad3564)
- Reinhold, T., Shapiro, A. I., Solanki, S. K., & Basri, G. 2023, *A&A*, 678, A24, doi: [10.1051/0004-6361/202346789](https://doi.org/10.1051/0004-6361/202346789)
- Rowan, D. M., Jayasinghe, T., Stanek, K. Z., et al. 2023, *MNRAS*, 523, 2641, doi: [10.1093/mnras/stad1560](https://doi.org/10.1093/mnras/stad1560)
- Santos, A. R. G., García, R. A., Mathur, S., et al. 2019, *ApJS*, 244, 21, doi: [10.3847/1538-4365/ab3b56](https://doi.org/10.3847/1538-4365/ab3b56)
- Sethi, R., & Martin, D. V. 2024, *Tight stellar binaries favour active longitudes at sub- and anti-stellar points*, <https://arxiv.org/abs/2403.03065>
- Shappee, B. J., Prieto, J. L., Grupe, D., et al. 2014, *ApJ*, 788, 48, doi: [10.1088/0004-637X/788/1/48](https://doi.org/10.1088/0004-637X/788/1/48)
- Simonian, G. V. A., Pinsonneault, M. H., & Terndrup, D. M. 2019, *ApJ*, 871, 174, doi: [10.3847/1538-4357/aaf97c](https://doi.org/10.3847/1538-4357/aaf97c)
- Skrutskie, M. F., Cutri, R. M., Stiening, R., et al. 2006, *AJ*, 131, 1163, doi: [10.1086/498708](https://doi.org/10.1086/498708)
- Skumanich, A. 1972, *ApJ*, 171, 565, doi: [10.1086/151310](https://doi.org/10.1086/151310)
- Strassmeier, K. G. 2009, *A&A Rev.*, 17, 251, doi: [10.1007/s00159-009-0020-6](https://doi.org/10.1007/s00159-009-0020-6)
- Tayar, J., Ceillier, T., García-Hernández, D. A., et al. 2015, *ApJ*, 807, 82, doi: [10.1088/0004-637X/807/1/82](https://doi.org/10.1088/0004-637X/807/1/82)
- Wilson, O. C. 1966, *ApJ*, 144, 695, doi: [10.1086/148649](https://doi.org/10.1086/148649)

This paper was built using the Open Journal of Astrophysics L<sup>A</sup>T<sub>E</sub>X template. The OJA is a journal which

provides fast and easy peer review for new papers in the **astro-ph** section of the arXiv, making the reviewing process simpler for authors and referees alike. Learn more at <http://astro.theoj.org>.